J. Biomed. Eng. Res.
Vol. 23, No. 3, 171-179, 2002

Three-Dimensional Kinematic Model of the Human Knee Joint during Gait

Joung Hwan. Mun* and Seichi Takeuchi+

*Department of Bio-Mechatronic Engineering, College of Life Science & Technology, Sungkyunkwan University
+Department of Electronic & Computer Engineering, Tokyo Denki University

(Received November 5, 2001. Accepted June 8, 2002)

요 약 : 운동 중에 있는 인체 무릎관절의 기능을 이해하기 위한 기구학적(Kinematic) 분석 과 동역학적(Kinetic) 분석을 행하는데 있어서, 관절 표면의 기하학이 주요한 역할을 한다는 것은 잘 알려져 있다. 슬관절은 미끄러짐 (sliding)과 구름 (rolling) 운동을 고려하지 않고는 정확하게 모델 될 수 없다.
본 연구에서는 미끄러짐 과 회전 운동 그리고 주요 인대 (ligament)를 고려한 3차원 인체 슬관절 모델을 제시한다. 본 연구는, 슬관절의 전형적인 측 평면 CT 영상의 확장으로부터 얻어진 두개의 캠 측면도를 이용하여 보다 실제에 가까운 관절의 기하학을 이용한 모델을 제시한다. 개발된 모델은 보행 중 인체 슬관절을 통한 힘의 전달경로를 예측하는데 있어서, 실험을 기초로 한 이전의 결과보고와 비교하여 볼 때 매우 잘 일치한다. 대퇴골와 경골 사이의 접촉 점은 무릎의 굽힘이 진행되는 동안 전방에서 후방으로 이동하는데 이것은 무릎의 굽힘과 폄의 운동에 대한 전방/후방 운동의 커플링을 반영한 것이다. 본 연구에서 개발된 모델에 의하면, 일회의 보행 사이클동안 경골 표면에 접촉 점의 전방/후방 이동변위는 바깥쪽 관절구 쪽이 약 16 mm 이고, 안쪽 관절구 쪽이 약 25 mm 이다. 또한, 일회의 보행 사이클 동안 대퇴골 의 이동변위는 바깥쪽이 약 7 mm 그리고 안쪽이 약 10 mm 이다. 개발된 모델은, 관절의 퇴화를 진단 하는데 이용할 수 있는 가능성이 기대된다.

Abstract : It is well known that the geometry of the articular surface plays a major role in the kinematic and kinetic analysis to understand human knee joint function during motion.
The functionality of the knee joint cannot be accurately modeled without considering the effects of sliding and rolling motions. We present a 3-D human knee joint model considering sliding and rolling motion and major ligaments. We employ more realistic articular geometry using two cam profiles obtained from the extrusion of the sagittal plain view of the representative Computerized Tomography image of the knee joint compared to the previously reported model. Our model shows good agreement with the already reported experimental results on prediction of the lines of force through the human joint during gait. The contact point between femur and tibia moves toward the posterior direction as the knee undergoes flexion, reflecting the coupling of anterior and posterior motion with flexion/extension. The anterior/posterior displacement of the contact point on the tibia plateau during one gait cycle is about 16 mm. for the lateral condyle and 25 mm. for the medial condyle using the employed model. Also, the femur motion on the tibia undergoes lateral/medial movement about 7 mm. and 10 mm. during one gait cycle for the lateral condyle and medial condyle, respectively. The developed computational model maybe potentially employed to identify the joint degeneration.

Key words : Gait analysis, Human motion, Joint degeneration, Biomechanics, Kinematics

INTRODUCTION

The human knee joint has been addressed in the literature because of its clinical importance and injuries due to the frequent ligament injures and osteoarthritis disease[1]. The articular geometry of the tibiofemoral condyle and the surrounding capsule ligamentous constraints directly affect the articular surface motion of the knee joint during motion. The functionality of the knee joint cannot be accurately modeled without considering the effects of sliding and rolling motion between the femur and the tibia. The kinematics of the joint cannot be modeled as a point contact, a hinge joint as one degrees-of-freedom(DOF), a universal joint(two DOF) or a spherical joint(three DOF) but has to take into consideration both sliding and rolling motions. Indeed, many studies have addressed the human knee joint using a single point-of-contact with two or three degrees-of-freedom[2-4] or by using two spherically shaped balls with fixed radii[1,5,6]. These models are faced with complexity in computation and equation formulation resul-

통신저자 : Joung Hwan. Mun, Ph.D. Department of Bio-Mechatronic Engineering College of Life Science & Technology Sungkyunkwan University Chunchun, Jangan, Suwon, Kyunggi, 440-746, KOREA
Tel. (031) 290-7827, Fax. (031) 290-7830

ting from the complex geometry of the articular joint in the knee. The redundancy of muscle and ligaments leads to further complications.

Wilson and O'Connor[1] reported a three-dimensional geometric model of the knee joint in gait analysis to predict the kinematics of the knee from the geometry of its anatomical structures using the rigid femur and tibia segment. They addressed two important problems related to the knee joint biomechanics such as the determination of the changing axis of rotation, and prediction of the lines of force through the major ligaments and femoral articulated surface. However, their geometric model was composed of rigid spherical surfaces that include much error in prediction the position and lines of action of the contact forces. Furthermore, kinematic locking occurred for joint angles greater than 60 degree due to the geometric simplification.

More recently, Abdel-Rahman and Hefzy [6] presented a 3-D human knee joint model undergoing impact loading. The model was composed of two-body segments, the femur and tibia, in contact, with the joint ligaments represented as nonlinear elastic springs. Major limitations of the model are that first, the external force applied on the tibia is a sinusoidal impacting load that is not applicable for general 3-D human locomotion. Thus, the computational model they developed cannot be applicable for understanding more standard activities where dynamic axial compressive forces act on the joint such as gait. Second, the medial and lateral articular surfaces were approximated as parts of spheres. However, since the geometry of the articular surface plays a major role in the kinematic and kinetic analysis of the dynamic knee joint model, more detailed geometry should be considered.

The objects of this study are : (1) to demonstrate a new knee joint model considering sliding and rolling motion and major ligaments and, (2) to predict the line of force through the human articular knee joint using inverse kinematics and contact modeling to understand human knee joint function during gait.

METHODS

In this study, the articular geometry was more accurately represented using two cam profiles obtained from the extrusion of the sagittal plain view of a representative Computarized Tomography(CT) image of the knee[7] as shown in Fig. 1. In addition, the previously reported statistical data reduction method[8] was adopted for the kinematic analysis of the invariable knee joint.

1. Kinematics of the Human Knee Joint Contact Model

We introduce a model of the human knee joint that can account for four possible contacts such as one point contact, two points contact, separation, and penetration. Our model is a 6 degree-of-freedom (DOF) knee joint represented by two digitized cam profile spheres consi-

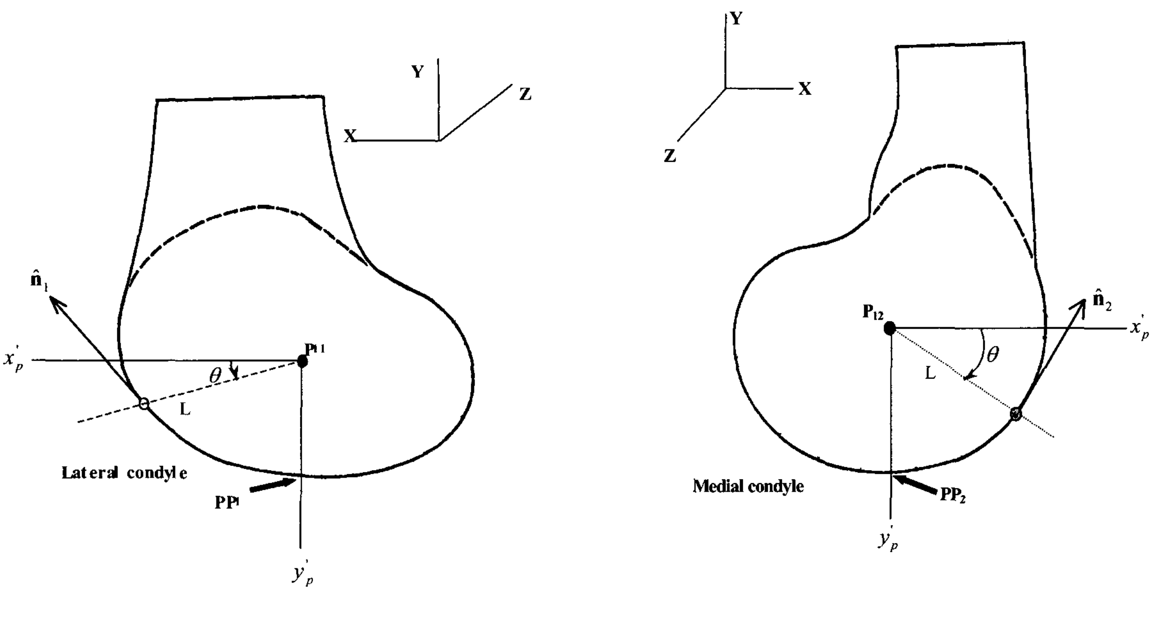

Fig. 1. The coordinate system of the digitized Lateral and Medical Condyle Contact Points

dering sliding and rolling as shown in Figures 1 and 2 with major ligaments as illustrated in Figures 6 and 7. In this study, we present the kinematic analysis needed to predict the lines of force through the articular surface at the human knee joint during locomotion. In the computational model, since the possibility of penetration and separation of the tibio-femoral joint while in motion is allowed, the system of constraint equation is assembled by only driving constraints as

$$\Phi(q\,t) = [\,\Phi^{D}(q,\,t)\,]_{nc} = 0 \tag{1}$$

,where D and nc represent the driving constraints and the number of constraints, respectively.

With a maximal set of Cartesian generalized coordinate, q={x_1, y_1, z_1, x_2, y_2, z_2, x_3, y_3, z_3, x_4, y_4, z_4, x_5, y_5, z_5, x_6, y_6, z_6}^{T}, the driving constraint equations are

$$\Phi_1^D = \begin{pmatrix} x_1 & -x_1^* \\ y_1 & -y_1^* \\ z_1 & -z_1^* \end{pmatrix} = 0 \tag{2}$$

$$\Phi_2^D = \begin{pmatrix} x_2 & -x_2^* \\ y_2 & -y_2^* \\ z_2 & -z_2^* \end{pmatrix} = 0 \tag{3}$$

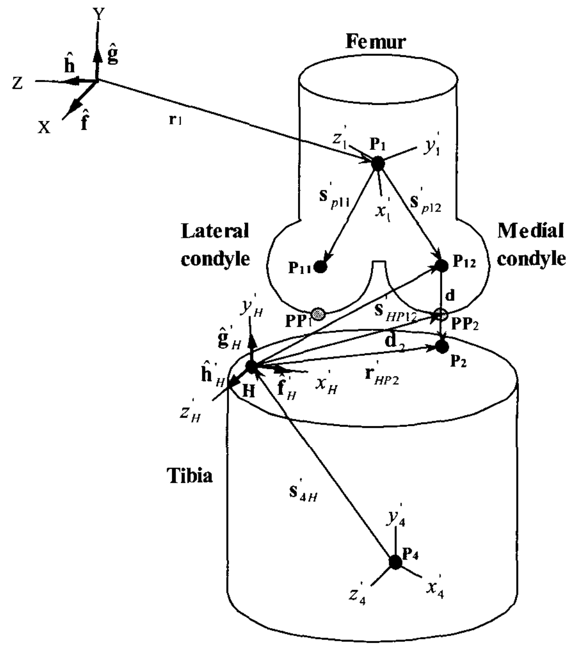

Fig. 2. The Configuration of the Knee Joint Contact Modeling

$$\Phi_3^D = \begin{pmatrix} x_3 & -x_3^* \\ y_3 & -y_3^* \\ z_3 & -z_3^* \end{pmatrix} = 0 \tag{4}$$

$$\Phi_4^D = \begin{pmatrix} x_4 & -x_4^* \\ y_4 & -y_4^* \\ z_4 & -z_4^* \end{pmatrix} = 0 \tag{5}$$

$$\Phi_5^D = \begin{pmatrix} x_5 & -x_5^* \\ y_5 & -y_5^* \\ z_5 & -z_5^* \end{pmatrix} = 0 \tag{6}$$

$$\Phi_6^D = \begin{pmatrix} x_6 & -x_6^* \\ y_6 & -y_6^* \\ z_6 & -z_6^* \end{pmatrix} = 0 \tag{7}$$

where $P_1(x_1,\ y_1,\ z_1)$, $P_2(x_2,\ y_2,\ z_2)$ and $P_3(x_3,\ y_3,\ z_3)$ represent the maker positions on femur and $P_4(x_4,\ y_4,\ z_4)$, $P_5(x_5,\ y_5,\ z_5)$ and $P_6(x_6,\ y_6,\ z_6)$ are the marker positions on tibia, and the asterisk, *, represents the kinematic values recovered from cubic spline functions.

In Figure 2, the position vectors of the of two sphere centers P_{11} and P_{12} can be expressed in terms of the global Cartesian reference coordinate system as

$$P_{11} = \mathrm{r}_{1+A_1}\mathrm{S}'_{p11} \tag{8}$$

$$P_{12} = \mathrm{r}_1 + \mathrm{A}_1\mathrm{S}'_{p12} \tag{9}$$

r_1 is the vector from the origin of the global coordinate system to the local origin of femur segment and A_1 is the transformation matrix from the local coordinate system of the femur to the global coordinated system during the motion. The constant local vectors s_{p11} and are s_{p12} calculated from the calibration position as

$$s'_{p11} = A_{1s}^{-1}(\mathrm{r}_1 - P_{11}) \tag{10}$$

$$s'_{p12} = A_{1s}^{-1}(\mathrm{r}_1 - P_{12}) \tag{11}$$

where A_{1s}^{-1} is the inverse matrix of the transformation matrix A_{1s} calculated at the calibration data set.

In the development of the following computational model, the medial condyle and tibia plateau will be considered as the example. The lateral condyle side equations can be developed in the same method as the medical condyle side equations. An arbitrary point H, placed on the tibia surface, can be expressed as

$$H=r_4+A_2 s'_{4H} \tag{12}$$

where r_4 is the vector from the origin of the global coordinate system to the local origin of tibia segment and s_{4H} is a constant vector given in the segment"s local coordinate system. This vector can be calculated at the calibration position and characterized by

$$s'_{4H}=A_{2S}^{-1}(r_4-H) \tag{13}$$

,where A_{2s}^{-1} is the inverse matrix of the transformation matrix A_{2s} calculated at the calibration position.

The calculation procedure of the contact point of the medial condyle on the tibia plateau, P_2, is followed. The contact point P_2 can be expressed in terms of global Cartesian coordinate system as

$$P_2=H+A_2 C_0 \begin{Bmatrix} a \\ 0 \\ c \end{Bmatrix} \tag{14}$$

$$C'_0=A_{2S}^{-1} \tag{15}$$

, where C_0 is the constant transformation matrix between the marker number P_4 and position H at the calibration position. The scalar values, a and c, are the distance from position H to the contact point P_2 in terms of local coordinate system of x_H, y_H and z_H. The geometric compatibility condition is that the vector d has to be perpendicular to the unit vectors $\hat{f}$ and $\hat{g}$ to satisfy the contact condition. Thus, the dot product equations can be written as

$$d\cdot\hat{f}=d\cdot A_2\cdot C'_0\hat{f}_H{}'=0 \tag{16}$$

$$d\cdot\hat{h}=d\cdot A_2\cdot C'_0\hat{f}_H{}'=0 \tag{17}$$

,where d is the vector from the P_{12} to the contact point of the medial condyle on the tibia plateau, P_2. $\hat{f}$, $\hat{g}$ and $\hat{h}$ are unit vectors along the local coordinate system, respectively.

And, the scalar distances a and c can be determined as

$$a=\hat{f}(P_1-H)=\hat{f}^{T}A_2C_0^{1}\begin{Bmatrix} a \\ 0 \\ c \end{Bmatrix}=\begin{Bmatrix} 1 \\ 0 \\ 0 \end{Bmatrix}^{T} C_0'^{T}A_2^{T}C'_0\begin{Bmatrix} a \\ 0 \\ c \end{Bmatrix} \tag{18}$$

$$c=\hat{h}(P_1-H)=\hat{h}^{T}A_2C'_0\begin{Bmatrix} a \\ 0 \\ c \end{Bmatrix}=\begin{Bmatrix} 0 \\ 0 \\ 1 \end{Bmatrix}^{T} C_0'^{T}A_2^{T}A_2C'_0\begin{Bmatrix} a \\ 0 \\ c \end{Bmatrix} \tag{19}$$

Since separation and penetration is allowed in the computational knee joint model, there exist two contact points for medial condyle such as P_2 and PP_2 while in motion. Thus, the distance directly affects the calculation of internal reaction force of knee joint.

$$\text{distance} = \hat{g}_H'^{T} d_2 \tag{20}$$

$$\hat{g}'_H=\hat{h}'_H\times\hat{f}'_H \tag{21}$$

Since the geometry of contact area plays the major role to determine the lines of action of the forces, internal reaction force and moment and the position and orientation of the axis of rotation of the knee, the irregular shape of the outline of contacting bodies such as femoral condyle must be described numerically to get accurate results. The real geometry of the femoral condyle is that the radii of curvature increase gradually postero-anteriorly, from 17 to 38 mm. for the medial condyle and from 12 to 60 mm. for the lateral condyle. The spiral does not have only one center but a series of centers lying on a spiral. Therefore the curve of the condyles represents a spiral of a spiral [9]. In order to describe the lateral and medial condyle in a closed-form expression, a cubic interpolation spline function is used. If two cubic polynomials s_1 and s_2 are known, the continuity conditions at point 2 in Figure 3 are followed as:

$$S_1=S_2 \tag{22}$$

$$\frac{ds_1}{d\theta}=\frac{ds_2}{d\theta} \tag{23}$$

$$\frac{d^2s_1}{d\theta^2}=\frac{d^2s_2}{d\theta^2} \tag{24}$$

$$s_1=a_0+a_1\theta+a_2\theta^2+a_3\theta^3 \tag{25}$$

$$s_2=b_0+b_1\theta+b_2\theta^2+b_3\theta^3 \tag{26}$$

The origins of the local coordinate for lateral and medial condyle, P_{11} and P_{12}, are placed at 20.4 mm and 19.9 mm upward from the PP_1 and PP_2 with respect to global laboratory Y direction [10] at the calibration position, respectively, as shown in Figure 2. In order to determine the spline function of lateral medial condyle, the sagittal plane CT image is digitized as shown in Figure 1. Any contact point, PP_1 or PP_2, on the digitized femoral condyles in Figure 2, can be described with respect to the $x_p' - y_p'$ femoral local coordinate system. As an example, medial side contact point on the femur, PP_2, can be expressed as

$$PP_2 = P_{12} + A_1 A_{1S}^{-1} \begin{Bmatrix} L\cos\theta \\ L\sin\theta \\ 0 \end{Bmatrix} \quad (27)$$

, where A_{1s} is the transformation matrix from the femoral body segment's local coordinate system to the global coordinate system. Since the tangent vector, $\hat{n}$, to the curve at the each time frame represents the contact point on the curve, the tangent vector equations can be written as:

$$\frac{dx_p'}{d\theta} = -L\sin\theta + \frac{dL}{d\theta}\cos\theta \quad (28)$$

$$\frac{dy_p'}{d\theta} = -L\sin\theta + \frac{dL}{d\theta}\sin\theta \quad (29)$$

Thus,

$$\hat{n} = \begin{bmatrix} \frac{dx_p'}{d\theta} \\ \frac{dy_p'}{d\theta} \end{bmatrix} \quad (30)$$

2. Gait Experiments

Experimental gait data from ten normal, healthy males (29±5 years old, 76±7 Kg, and height 174±6cm) with a free walking speed of 1.4 m/sec was used as input for the inverse kinematic analysis. As shown in Figure 4, the thigh segment was tracked using a total of three markers, placed along the lateral thigh, spaced at approximately 15 cm intervals with the middle marker on a 5.5cm extension toward the outside of the sagittal plane. The shank segment was tracked using three markers placed along the tibia separated by approximately 15cm with the middle marker mounted on a 7cm extension toward the outside of the sagittal plane. The markers were tracked using an Optotrak motion analysis system(model 3020, Northern Digital, Waterloo, Ontario) at 60Hz. The subject walked along a 30m walkway which contained a 3m by 2m data collection volume with an estimated resolution accuracy of greater than 1mm in all directions. Marker data were filtered at 6Hz using a 4th order Butterworth filter.

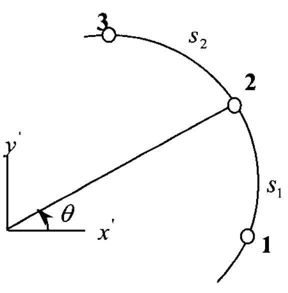

Fig. 3. Two cubic polynomials

MODEL VALIDATION

In order to verify the developed computational model with respect to kinematic analysis, the contact points between femoral condyle (lateral and medical condyle) and tibia surface are calculated using the one representative subject (29 years old, 76 Kg and height 175 cm) and compared with the previously reported experimental data based on the contact pressure measurement between in-vitro femoral condyle and tibial plateou using silicon rubber embossment during flexion/extension motion as shown in Figure 5(C). In Figure 5(A), contact point between femoral condyle, lateral and medial side, and tibia plateou on the tibia surface is presented with respect to local coordinate system. The relative motions between the

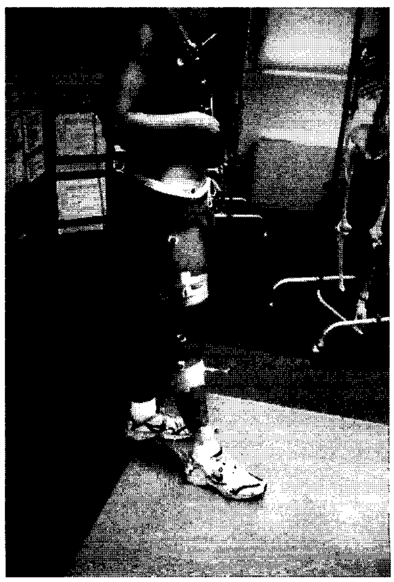

Fig. 4. Experimental anatomical marker system

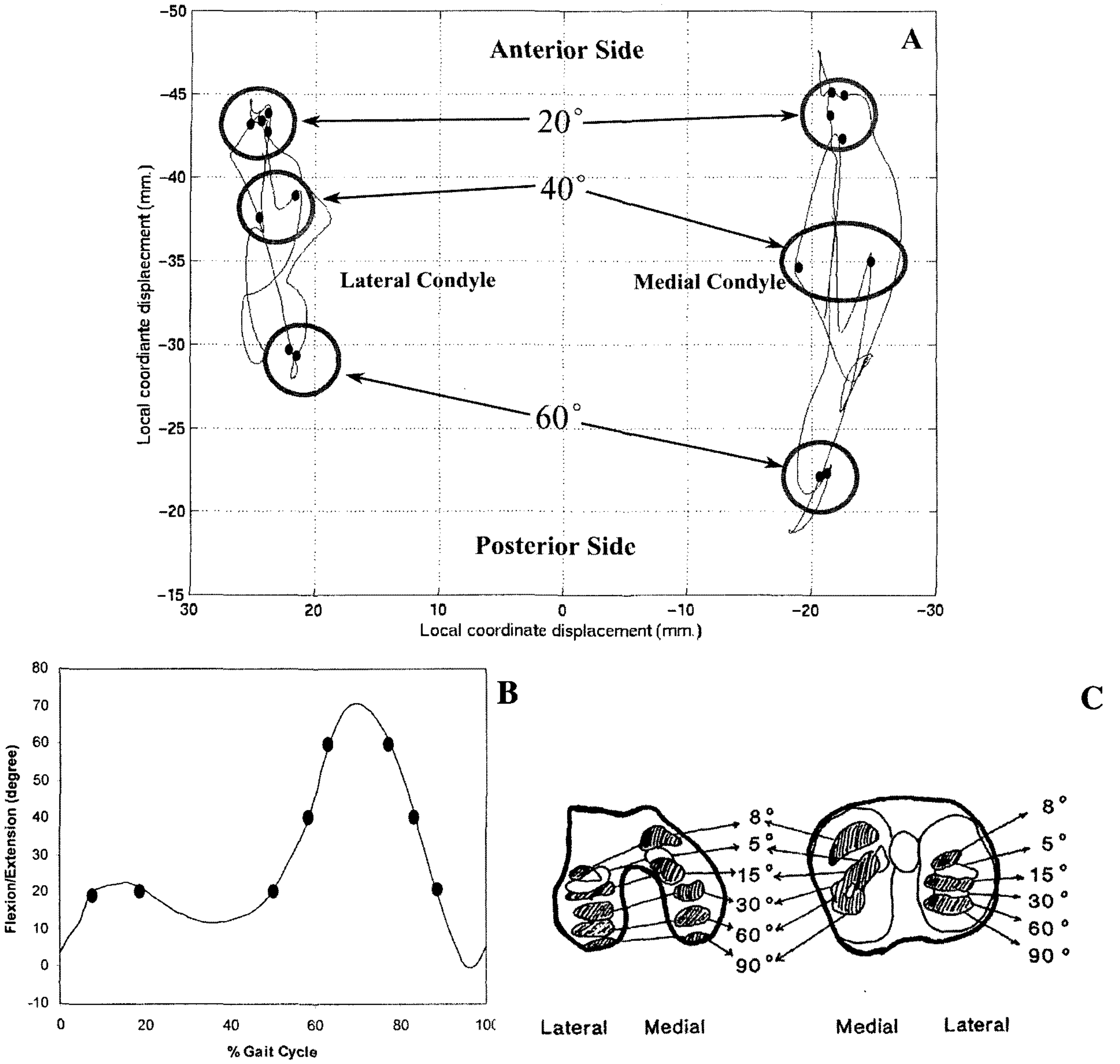

Fig. 5. (A) Tibio-femoral joint-articulating surface motion during human gait using improved kinematic contact model, (B) Flexion/Extension rotation angles during one gait cycle, (C) Tibio-femoral contact area

femur and tibia segments using Grood-Suntay's coordinate system[11] in terms of flexion/extension rotation is shown in Figure 5(B). As shown in Figure 5(A), the contact point undergoes sliding and rolling during one gait cycle. In addition, the femur and the tibia undergo 20o flexion/extension four times, 40o and 60o flexion/extension two times during one gait cycle as clearly seen in Figure 5(B). Thus, these corresponding frames are plotted, black round type dot, as shown in Figure 5(A). Following the figure, we can observe that the selected relative flexion/extension angles such as 20o, 40o and 60o, represented as the black round type dots, occurred closely each other. This implies the confidence of the developed computational model.

As observed in the previous studies[12,13], the contact point between femur and tibia moves in the posterior direction as the knee undergoes flexion, reflecting the coupling of antero-posterior motion with flexion/extension. The anterior/posterior displacement of the contact point on the tibia plateau during one gait cycle is about 16 mm. for the lateral condyle and 25mm. for the medial condyle based on the employed model if we assume that the representative cam profile for the femoral condyles and flat tibia plateau is employed in the model. Also, the

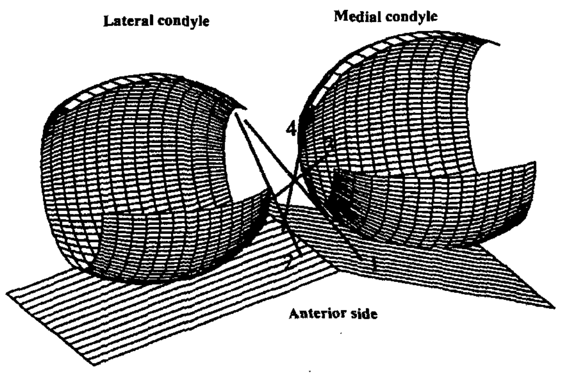

Number 1: Anterior fibers of the Anterior Cruciate (AAC)
Number 2: Posterior fibers of the Anterior Cruciate (PAC)
Number 3: Anterior fibers of the Posterior Cruciate (APC)
Number 4: Posterior fibers of the Posterior Cruciate (PPC)

Fig. 6. Cruciate ligaments at the knee joint

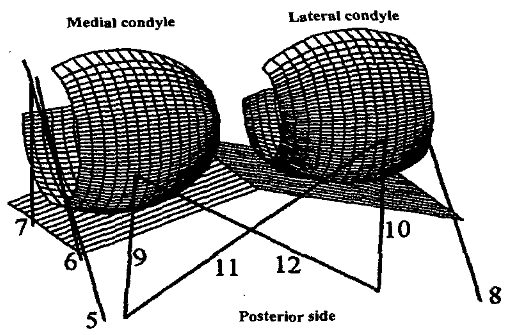

Number 5: Anterior fibers of the Medial Collateral (AMC)
Number 6: Oblique fibers of the Medial Collateral (OMC)
Number 7: Deep fibers of the Medial Collateral (DMC)
Number 8: Lateral Collateral (LCL)
Number 9: Medial fibers of the posterior Capsule (MCAP)
Number 10: Lateral fibers of the posterior Capsule (LCAP)
Number 11: Oblique Popliteal Ligament (OPL)
Number 12: Arcuate Popliteal Ligament (APL)

Fig. 7. Capsular ligaments at the knee joint

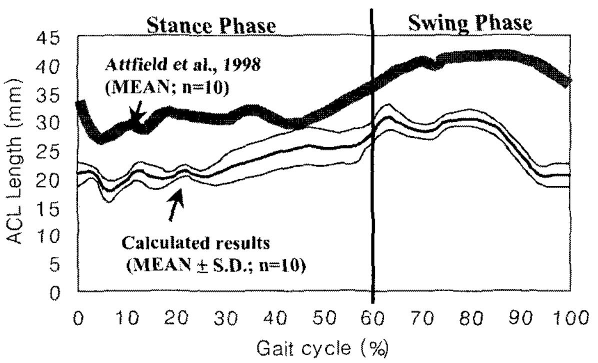

Fig. 8. Dynamic ACL length change during one gait cycle (n=10)

femur motion on the tibia undergoes lateral/medial movement by 7mm and 10 mm during one gait cycle for the lateral condyle and medial condyle, respectively. Thus, it is obvious that a fixed-point contact model using spherical joint or universial joint type cannot represent the knee motion properly.

In order to verify the generality of the model and to check the possibility of clinical application for the methodology developed in this study, Anterior Cruciate Ligaments(ACL) strain changes for the employed ten subjects at each time step has been calculated(Average+Standard Deviation) and compared to a previous study based on the experimental measurement of ACL strain during locomotion[14] from the ten normal healthy males as shown in Figure 8. In the developed computational model, twelve major cruciate and capsular ligaments were employed as shown in Figures 6 and 7. The coordinates of the origins and insertion points of the ligament bundle are adopted from published literatures[5]. The maximum ACL length was about 30mm occurred at 65% gait cycle which was just after the toe-off stage. As we can observe, the dynamic ACL length-changing pattern through one gait cycle in the previous study[14] is similar to our results.

DISCUSSION

In this study, we have presented a new knee joint computational model considering sliding and rolling motion and major ligaments for the prediction of the line of force through the human aricular joint during gait. The articular geometry was more accurately represented using two cam profiles obtained from the exclusion of the sagittal plain view of a representative CT image of the knee joint. The computer predicted contact points between femoral condyles and tibia surface moves from anterior side to posterior side as the knee undergoes flexion, reflecting the coupling of anterior and posterior motion with flexion/extension which had a good agreement compared with the previously reported experimental based results[13].

Iseki and Tomatsu[13] reported that the transposition of the tibio-femoral contact on the tibia is slightly greater in the lateral as compared with that of the medial during 30o to 90o of flexion. In addition, the medial tibio-femoral contact is gradually increased until the initial 25o flexion.

It is mainly due to the anatomical geometry of the human tibia plateau such as the difference of the curvature of bilateral femoral condyles, toe-in bilateral femoral condyles and convexity of lateral tibial plateau[13].

In the developed computational model, tibia plateau is assumbed to be a flat surface. In reality, the anatomical geometry of the human lateral tibial plateau is convex while the medial tibial plateau is concave shape. Thus, this anatomical simplification of the knee joint in the model causes the results that the medical condyle movement on the tibia surface is a little larger then the lateral condyle movement during whole gait cycle as shown in Figure 5(A). However, this result is reasonable under the assumption of a flat tibial surface since the transposition of the tibio-femoral contact on the femur is greater in the medial femoral condyle than in the lateral during one gait cycle[13].

In order to check the possibility of the clinical application for the developed computational model and methodology, we calculated dynamic ACL length change during one gait cycle for the employed ten healthy subjects as shown in Figure 8. The pattern during gait cycle was similar to the previously reported experimental results. However, we could observe that the magnitude of the ACL length is a little difference in terms of the magnitudes between our computational results and experimental results. We believe that this is mainly because of the simplicity of our computational model since our model doesn't consider the effects of patellar and the representative articular joint geometry and, ligament origin and insertion points in the developed computational model. In fact, the length of ACL is very short. Thus, little error in terms of the origin and insertion position of ACL led huge error for the strain calculation. However, these are not the limitation of the developed methodology since the developed equations and methods can be directly applicable to a computational model including more realistic geometry and more accurate origin and insertion position of ACL. In addition, the method and computational model developed in this study can be used to calculate more accurate predictions of both the femur position relative to the tibia and the axis of rotation of the knee compared to the previously reported computational model including the point contact at the human knee joint. Furthermore, it is directly applicable in a clinical gait analysis laboratory.

Several limitations in our computational model and the invoked assumptions need to be discussed. The developed computational model is composed of two rigid segments such as femur and tibia and twelve ligaments represented by nonlinear spring elements. In addition, representative geometry of the lateral and medial condyles, and ligament origin and insertion position are employed. Tibia surface is assumed to be flat [1]. Furthermore, a complete clinical comparison was not considered in this study.

The pattern of the ligament length change for the injured subject is expected to be different compared to the healthy subjects during human gait. Thus, the comparison of the dynamic strain using the developed computational model between the healthy and injured subjects should be observed in the future study. In addition, since accurate geometry of femoral and tibia condyles do major role to develop valuable computational model, the 3-D geometry model using interpolation method such as Non-Uniform spline Rational B-surfaces is recommended for the future study. Furthermore, accurate ligament origin and insertion position for the experimental subject should be determined to have more meaningful results of ligament function.

REFERENCES

1. D.R. Wilson and J.J. O'Connor, "*A Three-Dimensional Geometric Model of the Knee for the Study of Joint Forces in Gait*", Gait & Posture, Vol. 5, pp. 108-115, 1997
2. M.P. Kadaba, H.K. Ramakrishan and M.E. Wootten, "*Measurement of lower extremity kinematics during level walking*", Journal of Orthopaedic Research Society, Vol. 8, no. 3, pp. 383-392, 1990
3. B. Koopman, H.J. Grootenboer and H.J. de Jongh, "*An inverse dynamics model for the analysis, reconstruction and prediction of bipedal walking*", Journal of Biomechanics, Vol. 28, pp. 1365-1376, 1995
4. M.G. Pandy and N. Berme, "*A numerical method for simulating the dynamics of human walking*", Journal of Biomechanics, Vol. 21, no. 12, pp. 1043-1051, 1988
5. E.M. Abdel-Rahman : Three-dimensional dynamic anatomically based model of the human tibio-femoral joint, Ph. D. Thesis, University of Toledo, OH., 1995
6. E.M. Abdel-Rahman and M.S. Hefzy, "*Three-Dimensional Dynamic Behavior of the Human Knee Joint under Impact Loading*", Medical Engng. & Physics, Vol. 20, pp. 276-290, 1998
7. J.H. Mun, S.J. Song and J.S. Freeman, "*Improved contact model of the human knee joint during gait*", GCMA2000, Rochester, Minnesota, USA, 12-15, April,

2000

8. J.H. Mun, J.S Freeman and K. Rim, "*Human Gait Analysis Using Averaged Coordinate Reference System with Redundant Markers*", Gait & Posture, 2001.(Accepted for publication)
9. I.A. Kapandji, The Physiology of the Joints: Annotated Diagrams of the Mechanics of Human Joints, London, E.& S. Livingstone, 1970
10. H. Kurosawa, P.S. Walker, S. Abe, A. Grag and T. Hunter, "*Geometry and motion of the knee for implant and orthotic design*", J. Biomechanics, Vol. 18, pp. 487-499, 1985
11. E.S. Grood and W.J. Suntay, "*A joint coordinate system for the clinical description of three-dimensional motions: application to the knee*", J. of Biomechanical Engineering, Vol. 105, pp. 136-144, 1983
12. J.D. Bronzino, The Biomedical Engineering Handbook, Boca Raton; CRC Press; IEEE Press, 1995
13. F. Iseki and T. Tomatsu, "*The biomechanics of the knee joint with special reference to the contact area*", Keio J. Med. Vol. 25, pp. 37-44, 1976
14. S.F. Attfield, N.P. Gleeson, P. Pickering and D. Rees, "*Evaluation of dynamic anterior cruciate ligaments strain during ambulation*", Gait & Posture, Vol. 7, pp. 154-155, 1998
15. G.A. Ateshian, W.M. Lai, W.B. Zhu and V.C. Mow, "*An Asymptotic Solution for the Contact of Two Biphasic Cartilage Layers*", J. Biomechanics, Vol. 27, pp. 1347-1360, 1994
16. A. Cappello, A. Cappozzo, P.F.L. Palombara, L. Lucchetti, and A. Leardini, "*Multiple anatomical landmark calibration for optimal bone pose estimation*", Human Movement Science, Vol. 16, pp. 259-274, 1997
17. A. W. Eberhardt, L.M. Keer, J.L. Lewis and V. Vithoontien, "*An Analytical Model of Joint Contact*", J. Biomech. Engng., Vol. 112, pp. 407-413, 1990
18. A.W. Eberhardt, J.L. Lewis and L.M. Keer, "*Contact of Layered Elastic Spheres as a Model of Joint Contact: Effect of Tangential Load and Friction*", J. Biomech. Engng., Vol. 113, pp. 107-108, 1991